Radiation-induced reprogramming drives glioma vascular transdifferentiation and tumor recurrence

Sree Deepthi Muthukrishnan[1], Riki Kawaguchi[1], Pooja Nair[1], Rachna Prasad[1], Yue Qin[1], Maverick Johnson[1], Nathan VanderVeer-Harris[1], Michael C. Condro[1], Alvaro G. Alvarado[1], Raymond Gau[1], Qing Wang[1], Maria G. Castro[2], Pedro R. Lowenstein[2], Arjun Deb[3], Jason D. Hinman[4], Frank Pajonk[5], Terry C. Burns[6], Steven A. Goldman[7], Daniel H. Geschwind[1,4], Harley I. Kornblum[1,8,*]

[1]Department of Psychiatry and Behavioral Sciences, Semel Institute for Neuroscience & Human Behavior, David Geffen School of Medicine, UCLA, Los Angeles, CA, USA

[2]Department of Neurosurgery, University of Michigan Medical School, Ann Arbor, MI, USA

[3]Division of Cardiology, Department of Medicine, David Geffen School of Medicine, UCLA, Los Angeles, CA, USA

[4]Department of Neurology, David Geffen School of Medicine, UCLA, Los Angeles, CA, USA

[5]Department of Radiation Oncology, David Geffen School of Medicine, UCLA, Los Angeles, CA USA

[6]Department of Neurological Surgery, Mayo Clinic, Rochester, Minnesota, USA

[7]Center for Translational Neuromedicine, University of Rochester Medical Center, Rochester, NY, USA

[8]Department of Molecular and Medical Pharmacology, David Geffen School of Medicine, UCLA, Los Angeles, CA, USA.

Corresponding author: hkornblum@mednet.ucla.edu

Summary

Radiation-resistant glioma cells exhibit phenotypic plasticity leading to aggressive tumor recurrence. However, the underlying molecular mechanisms remain to be elucidated. Here, we employed single-cell and whole transcriptomic analyses to discover that radiation induces a dynamic shift in proportions and functional states of glioma cells allowing for acquisition of vascular- and mesenchymal-like phenotypes. The primary phenotypic switch induced by radiation is transdifferentiation of glioma cells to endothelial-like and pericyte-like cells. In turn, the transdifferentiated cells promote proliferation of radiated tumor cells, and their selective depletion results in reduced tumor growth post-treatment. The acquisition of vascular-like phenotype is driven by increased chromatin accessibility in vascular genes, and blocking P300-mediated histone acetyltransferase activity prior to radiation inhibits vascular transdifferentiation and tumor growth. Our findings indicate that radiation reprograms glioma cells driving vascular transdifferentiation and tumor recurrence, and highlights P300 HAT inhibitor as a potential therapeutic target for preventing GBM relapse.

Introduction

Glioblastoma (GBM) is a universally recurrent and lethal primary brain tumor characterized by extensive neovascularization, invasion into normal brain parenchyma, and marked resistance to chemo-radiation therapy (Aldape et al., 2019; Osuka and Van Meir, 2017). Within an individual GBM tumor, a small subset of neoplastic cells termed “glioma stem-like cells” (GSC) possess the capacity to self-renew and initiate tumor growth, multi-lineage differentiation and resistance to chemotherapy and radiation (Lathia et al., 2015; Prager et al., 2020). Prior studies have reported that the standard GBM treatments such as chemotherapy with Temozolomide (TMZ)- and radiotherapy-induced stress can lead to dedifferentiation of non-GSC tumor cells to a GSC-like state (Auffinger et al., 2014; Bhat et al., 2020; Dahan et al., 2014; Lee et al., 2016). GSC also exhibit robust developmental plasticity and transdifferentiation capacity. GSC and tumor

cells can switch between Proneural and Mesenchymal states driving invasion and resistance, and also transdifferentiate into vascular endothelial-like and pericyte-like cells contributing to tumor vascularization, growth and disease progression (Cheng et al., 2013; Minata et al., 2019; Neftel et al., 2019; Ricci-Vitiani et al., 2010; Yuan et al., 2019).

A growing body of evidence indicates that chemo- and radiation therapy can also induce proneural to mesenchymal-like transition and transdifferentiation to endothelial-like cells leading to aggressive tumor growth (De Pascalis et al., 2018; Deshors et al., 2019; Lau et al., 2015). However, it is unclear whether therapy can induce GSC transdifferentiation into pericyte-like cells, which are essential for maintenance of blood-tumor-barrier (Zhou et al., 2017). Although there is tremendous focus on illuminating the mechanisms underlying GSC heterogeneity in primary tumors, the precise molecular and epigenetic factors driving therapy-induced plasticity in refractory GSC and tumor cells in GBM recurrence remains to be elucidated.

In this study, we employed single-cell and whole transcriptomic analyses and chromatin accessibility profiling to determine the contribution of radiation therapy in reprogramming tumor cells to adopt diverse phenotypic cell states. We found that clusters expressing vascular/angiogenic and mesenchymal markers increase in size post-radiation, and are enriched for gene sets associated with angiogenesis and vascular development. Using patient-derived gliomasphere cultures, orthotopic xenograft and murine GBM models, we demonstrate that radiation induces transdifferentiation to both endothelial- and pericyte like- cells that in turn influence tumor growth. Importantly, we uncovered that radiation alters chromatin accessibility in some vascular genes resulting in their increased expression, and that the histone acetyltransferase (HAT) P300 is a key mediator promoting radiation-induced vascular transdifferentiation contributing to tumor relapse.

Results

Single-cell transcriptomics reveals a dynamic shift in cellular states of glioma cells post-radiation

To determine the contribution of radiation to phenotypic plasticity of glioma cells, we performed single cell RNA-sequencing (scRNA-seq) of a primary gliomasphere line exposed to a single dose of radiation at 8 Gy for 2- and 7-days. Integrated analysis of all the samples revealed 14 distinct clusters, a majority of which showed a dynamic shift in size (clusters 1, 2, 3, 5, 8, 10, 11), while a few increased (clusters 0, 4, 9) and some sharply reduced (clusters 6, 7, 12, 13) post-radiation (**Figure 1A,B**). For annotating clusters based on functional states, we performed an unbiased analysis using co-expressed gene networks and clustering by Louvain community detection. 29 gene-signature modules were identified that were differentially expressed between the 14 clusters. Gene ontology (GO) analysis of the modules using EnrichR database showed that clusters 6 and 7 that diminished post-radiation were enriched for mitosis and DNA-repair related processes. Interestingly, clusters 0 and 4 that increased in size post-radiation were highly enriched for embryonic development, vasculogenesis and mesenchymal stem cell differentiation modules, but show reduced expression of cell cycle and DNA-repair modules. Clusters 9 and 11 which also considerably increased in size after radiation were enriched for processes related to mitosis, cholesterol synthesis and embryonic development modules (**Figure 1C, Table S1**).

Next, we performed pseudotime trajectory analysis to determine the hierarchical sequence of these functional states. We *a priori* chose cluster 0 as an arbitrary starting point for constructing the trajectory. Predictably, the trajectory showed multiple branching events within and across clusters highlighting the heterogeneity of tumor cells (**Figure 1D**). By assigning the top highly enriched GO_terms for modules to their respective clusters on the trajectory, we found that the three previously described phenotypic states in glioma: GSC or stem-like, mesenchymal-like

and vascular-like states are represented in different clusters. To further verify this, we used previously validated markers for these cell states, and in addition, included lineage markers of neural crest/mesenchymal stem cells (NC-MSC) and mesodermal progenitor cells from which pericytes and endothelial cells are derived, respectively (Armulik et al., 2011; De Val and Black, 2009). Of the clusters that increase post-radiation, cluster 0 expressed markers of GSC, NC-MSC, mature pericyte markers and a few endothelial markers. Cluster 4 showed increased expression of some mesodermal, and many mature endothelial markers, and low levels of GSC and mesenchymal markers. While cluster 9 was enriched with mitotic gene module, it showed virtually no expression of GSC markers (**Figure S1A**). These results indicate that glioma cells in culture exist in diverse functional states, and a small fraction of radiation-resistant tumor cells in the gliomaspheres acquire the vascular, mesenchymal or stem-like states.

To examine if the *in vitro* cell states are replicated *in vivo*, we performed scRNA-seq on tumor cells isolated from radiated and control xenografts generated in NSG mice. Integrated analysis of the samples containing about 2000 control and 4000 radiated GFP+ tumor cells identified 15 clusters in total, of which clusters 1,2-4,9,10, 12 and 13 increased in frequency, and clusters 0, 5, 6,7 and 11 diminished in radiated tumors. **(Figure S1B,C**). Louvain community detection clustering and trajectory analysis showed that clusters with greater frequency in radiated tumors were enriched in adhesion/junction assembly, cGMP signaling, angiogenesis, EMT and migration-related processes. In contrast to *in vitro* findings, clusters that diminished in size expressed modules enriched in embryonic eye development, ion homeostasis, migration, and stem cell differentiation, and not cell-cycle, DNA-repair, or stress-response related processes (**Figure S1D,E, Table S1**). Using marker analysis, we found that clusters 4 and 9 had highest expression of GSC markers, and clusters 10 and 13 showed increased expression of mature endothelial markers. Clusters 1 and 15 that also increase in size in radiated tumors display high levels of NC-MSC and pericyte markers (**Figure S1F).** Together, these data indicate that

refractory tumor cells acquire endothelial and mesenchymal-like phenotypes in tumor xenografts, essentially replicating the *in vitro* findings.

Whole-transcriptomic sequencing confirms the enrichment of angiogenic and vascular markers in gliomaspheres post-radiation

Next, we sought to determine if radiation-induced functional states observed in single cell studies are discernible in patient-derived gliomasphere cultures by bulk RNA-sequencing. Hierarchical clustering of normalized gene expression showed that radiated cells at day 2 and day 7 clustered separately from each other, and from control cells **(Figure S1G,H).** As expected, gene set enrichment analysis (GSEA) showed enrichment of gene ontology (GO) terms related to radiation, and reduction in gene sets associated with cell cycle and DNA repair in both day 2 and day 7 radiated cells **(Figure 1E).** Furthermore, in line with single cell studies, we found enrichment of gene sets related to angiogenesis, embryonic development, neural crest stem cell and mesenchymal transition, and downregulation of proneural and neuronal gene sets in radiated gliomaspheres. Closer examination of the genes associated with these processes showed significant enrichment of vascular and angiogenesis genes (*p<0.05, Benjamini-Hochberg adjusted*), and a small subset of mesenchymal genes from the Verhaak_Glioblastoma_Mesenchymal geneset in 7-day radiated gliomaspheres (**Figure 1F, Figure S1I**). Quantitative RT-PCR and immunostaining confirmed the enrichment in vascular markers that included mature endothelial (PECAM1, CDH5, FLT1, EDN1) and pericyte (DES, ACTA2, MCAM, CD248) genes in day 7 radiated gliomaspheres (**Figure 1G, Figure S1J**). These markers were not significantly upregulated in day 2 gliomaspheres, corroborating the findings from bulk RNA sequencing. This data suggests that radiation promotes angiogenic and vascular gene expression in gliomaspheres.

Radiated glioma cells display enhanced endothelial and pericyte marker expression

Standard radiation therapy for GBM patients involves a fractionated dose regimen of 2 Gy for 30 days (Hingorani et al., 2012). However, our transcriptomic analyses were performed with a single high dose of radiation, 8 Gy. Therefore, we assessed whether fractionated radiation (2 Gy, x4) also induces vascular-like phenotypes in gliomaspheres. Quantitative RT-PCR analysis of both fractionated and single dose radiated gliomaspheres showed significant increase in endothelial and pericyte markers **(Figure 2A)**. We also found that the increase in vascular marker expression by radiation was not dose-dependent, and that both low (2 and 4 Gy) and high (8 and 10 Gy) dose were effective at inducing the expression of the majority of the vascular genes assessed (**Figure S2A**). Most GSC and mesenchymal markers were not significantly upregulated by fractionated and single-dose radiation **(Figure S2B)**, suggesting that radiation predominantly induces vascular cell-like state in primary gliomaspheres.

To determine the generalizability of our findings, we then used the single high dose 8 Gy to verify if radiation promotes vascular marker expression in multiple patient-derived gliomasphere lines that included the 3 molecular subtypes and both primary and recurrent IDH1-wild type and mutant GBM. We found significant upregulation of vascular markers, albeit to a varying degree, in all gliomasphere lines examined irrespective of the molecular subtype and mutational status. Interestingly, Proneural lines (HK_217, HK_408, HK_347) showed the highest expression for endothelial markers (PECAM1, CDH5), and the Mesenchymal lines (HK_372, HK_412, HK_308) exhibited the highest pericyte marker expression (DES, ACTA2). Although the primary GBM lines did not show an increase in GSC markers, some of the recurrent GBM lines showed an increase in GSC markers including SOX2, NANOG and OCT4 post-radiation **(Figure 2B).** To quantify the extent of radiation-induced vascular transdifferentiation, we generated lentivirus constructs containing endothelial (VE-CADHERIN/CDH5) or pericyte (DESMIN) promoter to drive expression of fluorescent mCherry reporter. We found that maximal reporter activation from both promoters occurs 3- and 7-days post-radiation **(Figure 2C, D).** Flow cytometric

analysis using previously validated endothelial (CD31, CD144) and pericyte markers (CD146, CD248) also showed increased percentage of double-positive cells 3- and 7-days post-radiation (**Figure S2).** Co-expression of both reporters showed that the majority of cells did not display overlapping expression of VE-CADHERIN-mCherry and DESMIN-GFP in both control and radiated gliomaspheres (**Figure S2C**). Immunostaining and qRT-PCR analysis of FACS sorted reporter-positive and negative fractions also indicated that endothelial and pericyte markers are expressed by distinct cells in gliomaspheres **(Figure S2D-F).**

To distinguish between the possibilities that radiation: a) induces vascular transdifferentiation vs b) promotes expansion of pre-existing transdifferentiated cells**,** we preemptively depleted the reporter positive cells by FACS. Radiation of reporter negative fractions activated both VE-CADHERIN and DESMIN reporters, but no activation was seen in non-radiated gliomaspheres (**Figure S2G,H**). We also extended these findings by examining reporter activation in multiple patient-derived gliomasphere lines. Interestingly, while gliomaspheres from the Proneural (PN) and Classical (CL) subtypes showed similar expression levels for both reporters, the Mesenchymal (MES) subtype showed significantly higher pericyte reporter expression compared to endothelial reporter (**Figure S4I**), indicating that glioma cells from specific molecular subtypes may exhibit differential propensity for transdifferentiation towards endothelial and pericyte-like states in response to radiation.

CD133+ glioma stem-like cells exhibit higher propensity for vascular transdifferentiation post-radiation

Prior studies have demonstrated that CD133+ GSC transdifferentiate into endothelial cells and pericytes (Cheng et al., 2013; Ming-Tsang Chiao et al., 2011; Ricci-Vitiani et al., 2010). To determine if radiation promotes vascular transdifferentiation in GSC or non-GSC tumor cells, we also utilized CD133 (PROM1) as the GSC marker to separate the stem-like fraction from non-

stem like cells (Brescia et al., 2013). Because this GSC marker is not informative in all cultures, we validated its significance in the cell line being used, HK_408 with limiting diluting assay and orthotopic transplantation of a small number (1000 cells) of CD133+ and CD133- cells into mice (**Figure S2J,K).** Radiation of either the CD133+ or CD133- fractions showed significantly increased endothelial and pericyte marker expression in the CD133+ GSC fraction at 3 and 7-days post-radiation. GSC markers were also highly upregulated in the CD133+ GSC fraction relative to CD133- tumor cells (**Figure 2E**). Immunostaining of endothelial (CD31/VE-CADHERIN) cells and pericyte (DESMIN/aSMA) markers, and reporter expression confirmed that GSC exhibit greater capacity for transdifferentiation than non-GSC in response to radiation (**Figure 2F,G**). These findings indicate, at least for this cell line, that radiation-induced vascular transdifferentiation is isolated to the stem cell fraction.

Radiation promotes vascular transdifferentiation in orthotopic xenograft and mouse GBM models

To determine if radiation promotes vascular transdifferentiation of glioma cells *in vivo*, we first generated orthotopic xenograft tumors using the gliomasphere line HK_408 infected with a Firefly-Luciferase-GFP lentivirus. Tumor-bearing mice were exposed to a single dose of 8 Gy radiation. Immunostaining for vascular markers showed an increase in tumor cells co-expressing GFP with VE-CADHERIN or CD31 (endothelial) and DESMIN or αSMA (pericyte) in radiated tumors, indicating that glioma cells transdifferentiated into vascular-like cells post-radiation *in vivo* (**Figure 2H and S2L**). To reliably measure *in vivo* vascular transdifferentiation, we generated xenografts with tumor cells transduced with VE-CADHERIN (CDH5-mC) and DESMIN (DES-mC) reporters. Tumor-bearing brains from control and radiated groups were harvested 2 weeks after radiation, and analyzed by immunostaining and flow cytometry for the presence of GFP+ mCherry+ cells (**Figure 2I**). Immunostaining for GFP (tumor) and mCherry (transdifferentiated cells) revealed an increase in co-labelled cells in radiated tumors, and flow

cytometric quantitation showed that this increase was significant for endothelial- (8% vs 2% control, * p<0.005) and pericyte- (13% vs 3% control, **p<0.005) like cells in radiated tumors (**Figure 2J).** These findings suggest that radiation indeed promotes glioma transdifferentiation into both endothelial-like and pericyte-like cells *in vivo*.

Next, we asked whether the presence of an intact immune system affects transdifferentiation capacity of glioma cells post-radiation in a syngeneic mGBM model (Núñez et al., 2019). We first verified that mGBM cultures showed enrichment of vascular genes post-radiation (**Figure S2M)**. Examination of tumors showed that there was co-staining of GFP (tumor cells) with endothelial (VE-CADHERIN) and pericyte (DES) markers post-radiation Quantification of GFP+ marker+ cells revealed that there was significant increase in transdifferentiated vascular-like cells in the blood vessels as well as in the tumor mass in radiated mice **(Figure 2K,L).** This indicates that radiation-induced vascular transdifferentiation is not inhibited by an intact immune microenvironment as would exist in human tumors.

Radiation-induced glioma endothelial cells (iGEC) exhibit characteristics of normal vascular endothelial cells

Typically, the identity and behavior of normal vascular endothelial cells (VEC) is ascertained by their ability to uptake labelled low-density lipoproteins (LDL) and form tubular networks on GFR-Matrigel mimicking the blood vessels (Alexander et al., 1991; DeCicco-Skinner et al., 2014; Francescone et al., 2011). Earlier studies have shown that glioma-derived endothelial cells possess these characteristics (Ricci-Vitiani et al., 2010; Soda et al., 2011; Wang et al., 2010). We therefore asked if radiation-induced glioma endothelial cells, referred to henceforth as "*iGEC*" also exhibit characteristics of normal VEC. We used human umbilical vein endothelial cells (HUVEC) as a reference for normal VEC to assess these phenotypes. Similar to HUVEC,

radiated glioma cells also showed tubular-network formation on Matrigel, and increased uptake of DiI-Ac-LDL compared to non-radiated cells (**Figure 3A-D, Figure S3A,B**).

We next performed Matrigel plug *in vivo* angiogenesis assay using FACS sorted reporter-negative tumor cells (mCherry-) and or reporter-positive iGEC or nGEC (CDH5-mCherry+) to determine if they integrate into host vasculature or induce angiogenesis when embedded subcutaneously (**Figure 3E**). Histological examination with hematoxylin & eosin (H&E) and Masson's Trichrome staining revealed vessel formation in both GBM and GEC-embedded plugs. Immunostaining revealed some mCherry+ cells lining along the vessels labelled with Tomato Lectin only in iGEC and nGEC groups indicating that some transdifferentiated vascular cells may integrate into host vasculature (**Figure 3F)**. Quantitation of Trichrome stained sections also showed that both iGEC and nGEC groups had significantly higher vascular density than their corresponding tumor fractions (**Figure 3G**).

To validate that the angiogenic and vascular gene signatures are restricted to transdifferentiated cells, and that they are molecularly distinct from the rest of the tumor cells, we performed RNA-sequencing on sorted reporter+ (iGEC/GPC and nGEC/GPC, mCherry+) and reporter-(mCherry-) tumor cells from control and radiated gliomaspheres. Multi-dimensional scaling (MDS) and hierarchical clustering of gene expression showed that tumor cells and transdifferentiated vascular-like cells clustered separately (**Figure 3H**). Differential gene expression analysis also revealed significant number of up and down-regulated genes between tumor versus transdifferentiated cells (**Figure S3C**). Examination of canonical endothelial (CD31 and VE-CADHERIN) and pericyte (DES and ACTA2) markers confirmed the enrichment of these transcripts in GEC and GPC fractions, respectively (**Figure S3D**). GSEA also showed increase in vasculature and angiogenesis related gene sets in GEC and GPC fractions compared to their respective tumor fractions (**Figure 3I**). GPC fractions were also enriched for

smooth muscle- and mesenchymal-gene signatures consistent with their mesenchymal identity (**Figure 3I)**. We also observed downregulation of stem cell, neuronal, glial and nervous system development-related gene sets in the transdifferentiated cell fractions relative to tumor cells, further confirming that the transdifferentiated cells are molecularly distinct from their precursor tumor cells, and exhibit some vascular-like characteristics.

iGEC and iGPC promote growth of radiation-resistant tumor cells

Given that only a small number of GEC and GPC contribute to vascular structure formation, we asked whether they provide trophic support to promote tumor growth following treatment. To test this, we first collected conditioned media (CM) from the sorted and cultured non-induced (nGEC/nGPC) and induced (iGEC/iGPC) vascular-like cells (**Figure 4A**). Addition of CM from iGEC/GPC to radiated tumor cells significantly promoted their proliferation, whereas it did not show significant growth promoting effect on non-radiated tumor cells (* $p<0.05$, N=4, one way-ANOVA). CM from unsorted GBM cells did not promote growth of radiated tumor cells (**Figure 4B**). We also performed this assay on control and radiated tumor cells isolated from tumor xenografts, and obtained similar results, confirming that the transdifferentiated cells can provide trophic support to treatment-resistant tumor cells to promote their growth (**Figure S4A**).

To demonstrate the trophic function of iGEC and iGPC *in vivo*, we employed two complementary strategies. First, we performed co-transplantation of control and radiated reporter-negative tumor cells with their respective GEC and GPC fractions in a 1:1 ratio, and assessed tumor growth at 2 and 4 weeks after transplantation (**Figure 4A**). Remarkably, co-transplanted iGEC and iGPC significantly enhanced the growth of radiated tumor cells (reporter, mC^-) compared to tumor cells only, corroborating the *in vitro* findings (**Figure 4C,D and Figure S4B**). Survival analysis also showed that the co-transplanted mice exhibited signs of morbidity significantly earlier than mice transplanted with tumor cells alone **(Figure 4E).**

Next, we performed selective depletion of iGEC/GPC *in vivo* using the HSV-TK-Ganciclovir cell ablation strategy by driving expression of HSV-TK under the control of either VE-CADHERIN (CDH5-HSVTK-mCherry) or DESMIN (DES-HSV-TK-mCherry) (**Figure 4F**). After verifying tumor formation, mice were radiated with a single dose of 8 Gy, and injected with GCV every day for one week to allow depletion of reporter+ cells expressing HSV-TK. Quantification of tumor growth pre- and post-radiation and GCV administration revealed that depletion of either iGEC and iGPC significantly reduced tumor growth after radiation (**Figure 4G,H**). On the other hand, depletion of nGEC and nGPC did not show a significant effect on non-radiated tumors. We also did not see growth inhibition on tumors transduced with reporter constructs lacking HSV-TK when administered with GCV indicating that only transdifferentiated cells expressing HSV-TK were selectively depleted resulting in growth inhibition **(Figure S4C,D).** We also utilized another cell ablation strategy by expressing Diphtheria Toxin Receptor (DTR) to selectively deplete transdifferentiated cells. Since human cells are known to express the DT receptor, HB-EGF we first ensured that the protein is not expressed by our cell line, and also verified that Diphtheria toxin (DT) treatment selectively ablated the DTR-expressing cells (Figure S4E-F). Similar to HSV-TK depletion, mice-bearing tumors were radiated and administered with DT in 3 doses over the course of one week to ablate GEC/GPC **(Figure S4G)**, and found significant inhibition in tumor growth (**Figure S4H-J**). Collectively, the *in vitro* and *in vivo* findings strongly suggest that transdifferentiated vascular-like cells provide trophic support to tumor cells and promote recurrence after radiation.

Radiated gliomaspheres exhibit increased chromatin accessibility in vascular genes

Transition between cellular states requires epigenetic and transcriptional reprogramming mediated by alterations in chromatin structure and accessibility (Reik et al., 2001; Suvà et al., 2013). We therefore asked whether radiation-induced vascular transdifferentiation involves

changes in chromatin accessibility, especially in vascular genes or in regions that are bound by vascular specification factors. To test this hypothesis, we performed ATAC-sequencing on control and radiated gliomaspheres 2-days post-radiation. We chose the 2-day time point to determine the earliest changes that occur in the surviving fraction of tumor cells immediately after radiation-induced damage, and prior to significant induction of vascular marker expression. Notably, we found a small increase in peak count (open regions) in radiated tumor cells, and these peaks were largely localized to intergenic and intronic regions (**Figure 5A-C, Figure S5A**). Principal component analysis (PCA) of all the peaks showed distinct clustering of radiated and control gliomaspheres (**Figure S5B**). GO analysis of peaks specific to and shared between control and radiated gliomaspheres showed enrichment of embryonic development-related processes in radiated cells, whereas cell cycle/mitosis, regulation of transcription and translation-related processes were shared between the two groups (**Figure S5C**).

Next, we specifically examined if chromatin accessibility increased in vascular genes in radiated cells allowing for their increased expression. We found significant increase in peak size in regions upstream of the promoter as well as in intergenic regions of endothelial (VE-CADHERIN /CDH5, CD31/PECAM1) and pericyte (ANGPT1, MCAM) genes (**Figure 5D**). We then conducted differential analysis of all the peak regions for binding sites for transcription factors (TF), and found significant enrichment of motifs associated with vascular specification in radiated cells (**Figure 5E, F)**. Importantly, GO analysis of all the differentially open peaks revealed enrichment of GO terms associated with angiogenesis, vascular development and endothelial cell fate commitment and differentiation in radiated cells (**Figure 5G, Table S2**). These results from *in vitro* cultures indicate that radiation-resistant tumor cells display increased accessibility in regions associated with vascular genes allowing their increased expression.

Blocking P300 histone acetyltransferase activity inhibits vascular transdifferentiation

Histone acetylation is a major determinant of chromatin accessibility (Bannister and Kouzarides, 2011; Görisch et al., 2005). We wondered whether radiation alters histone acetylation levels leading to changes in chromatin accessibility in vascular genes. To address this, we performed immunoblotting for total and acetylated histone levels at different time points after radiation in gliomaspheres. Intriguingly, we saw that the total histone 3 (TH3) levels reduced at 6 hrs, but increased around 24-48 hrs post-radiation. We also observed a corresponding change in acetylated histone 3 (Ac-H3) levels with radiation (**Figure 6A**). Quantitation revealed a significant difference in Ac-H3 and TH3 in radiated tumor cells (**Figure 6B**). To further verify this, we conducted immunostaining for total and Ac-H3 in radiated and control tumor sections from orthotopic xenografts. Qualitatively and quantitatively, we found significant reduction in total H3 positive tumor cells, and on the other hand, a significant increase in Ac-H3 positive cells (**Figure 6C,D**). We also examined radiated and control mGBM tumors and found significant increase in Ac-H3 positive tumor cells post-treatment **(Figure S6A,B).**

Next, we sought to determine whether blocking histone acetylation prior to radiation inhibits vascular transdifferentiation. First, we examined our RNA-seq data to determine which histone acetyltransferases (HATs) are expressed in radiated tumor cells. Of the 14 known HATs, the EP300 and KAT2B HAT transcripts showed uniform expression in radiated tumor cells at both 2 and 7-days post-treatment. (**Figure 6E**). EP300 was enriched not only in tumor cells, but also in GEC and GPC **(Figure S6C**). Therefore, we decided to target the HAT activity of P300 using a selective small molecule inhibitor, C646 (Bowers et al., 2010). We validated the inhibitor by examining its effect on AcH3 by immunoblotting (**Figure 6F**). Quantitative RT-PCR analysis of endothelial and pericyte markers showed significant downregulation in combined C646 and radiation-treated gliomaspheres compared to radiation treatment alone (**Figure 6G**). This inhibitory effect was seen in two other GBM lines as well as the murine GBM model **(Figure S6D-F).** We also found significant inhibition of radiation-induced vascular marker expression in

CD133+ GSC fraction with C646 treatment **(Figure 6H and Figure S6G).** Furthermore, we utilized the endothelial (CDH5-mCherry) and pericyte (DES-mCherry) reporters and determined that pre-treatment with C646 significantly reduced the expression of the reporters in response to radiation in gliomaspheres, as well as in sorted CD133+ GSC fraction (**Figure 6I,J and Figure S6H, I**). We also performed RNA-sequencing on cells treated with radiation alone or combined C646 + radiation treatment and control cells. Treatment with C646 significantly changed gene expression in control and radiated cells **(Figure S6J,K),** and more importantly, reduced the expression of several vascular genes induced by radiation **(Figure 6K).** This is also reflected in GSEA where gene sets related to vascular development, angiogenesis, and mesenchymal transition are diminished, and those associated with DNA repair were enriched (**Figure 6L,M**). Together, these data suggest that P300-mediated histone acetylation plays a key role in promoting radiation-induced vascular transdifferentiation.

EP300-deficient cells show reduced vascular transdifferentiation and tumor growth post-radiation

To verify that P300-mediated histone acetylation is essential for radiation-induced vascular transdifferentiation *in vivo*, we utilized lentiviral-siRNA to knockdown EP300 in gliomaspheres. The knockdown efficiency was verified by quantitative RT-PCR analysis of EP300 transcript and immunostaining for P300 protein (**Figure S7A, B**). EP300-deficient cells (siEP300) also showed reduced AcH3 compared to control (SiCTL/Scrambled) cells (**Figure 7A, B**). As expected, and in line with the C646 inhibitor studies, EP300-deficient cells also showed reduced expression of endothelial and pericyte genes and reporter activation in gliomasphere cultures post-radiation (**Figure 7C-E, Figure S7C)**. Finally, we generated tumor xenografts with EP300-deficient and CTL cells and subjected them to radiation. EP300-deficient cells showed significant reduction in tumor growth post-treatment and increased animal survival (**Figure 7F,G**). Immunostaining for total and AcH3 showed fewer AcH3-positive tumor cells with EP300 knockdown, and

quantitation revealed that this reduction was significant in radiated, EP300-deficient tumors **(Figure S7D,E).** We also performed immunostaining and quantitation of endothelial (VE-CADHERIN/CD31) and pericyte (DESMIN/aSMA) marker expression in tumor cells (GFP) and observed a significant reduction in radiated EP300-deficient tumors compared to radiated and untreated EP300-deficient or control tumors **(Figure 7H,I and Figure S7F,G).** In summary, these findings indicate that P300-mediated histone acetylation significantly contributes to the radiation-induced vascular-like transdifferentiation of glioma cells.

Discussion

There is no standard of care treatment for recurrent GBM; and re-irradiation, chemotherapy or surgery only offer palliative care in managing the disease and fail to improve overall patient survival. A major challenge in developing therapies for recurrent GBM is the molecular heterogeneity and phenotypic plasticity of treatment-refractory tumor cells. Understanding the cellular and molecular mechanisms by which radiation therapy drives phenotypic plasticity and tumor aggressiveness can have profound implications for treating recurrent GBM.

In this study, we show at the single-cell level that radiation significantly alters the proportions and functional states of glioma cells. Primarily, radiation-induces the transdifferentiation of CD133+ GSC and tumor cells into endothelial-like and pericyte-like cells, which in turn provide trophic support to the radiated tumor cells and promote tumor growth and recurrence. Radiation likely induces the vascular-like phenotype by promoting increased accessibility of the chromatin in vascular gene regions leading to their increasing expression. This phenotypic switch can be blocked by inhibiting the HAT activity of P300, which highlights a key role for HAT in regulating radiation-induced plasticity and as a potential target for preventing tumor relapse in GBM.

GSC transdifferentiation to vascular endothelial-like cells and pericytes has been controversial for several reasons: 1) their close proximity 2) shared markers 3) frequency and function in primary tumors (higher numbers of GPC) (Armulik et al., 2005; Cheng et al., 2013). While both the cell types are essential for neovascularization, maintenance of blood-tumor-barrier and disease progression, their relative numbers suggest that they may arise from different sub populations of GSC or tumor cells (Soda et al., 2011; Wang et al., 2010; Zhou et al., 2017). Indeed, recent studies have found higher numbers of GEC in recurrent tumors compared to matched primary tumors, indicating that their frequency may vary pre- and post-treatment (De Pascalis et al., 2018; Hu et al., 2016). Our findings that radiation-induces transdifferentiation of tumor cells to an endothelial-like state reinforces these studies and provides additional evidence that they may be found in greater frequency in recurring GBM tumors post-treatment.

Radiation-therapy has been shown to promote Proneural to Mesenchymal-like conversion of GSC, which leads to increase tumor invasion (Bhat et al., 2013; Minata et al., 2019). However, it was unclear whether radiation-induced mesenchymal conversion is associated with pericyte-like state or that it alters their frequency in tumors. Pericytes in brain are derived from neural crest-mesenchymal stem cells (NC-MSC) (Armulik et al., 2011). In our single-cell analysis, we identified a cluster distinct from EC-like cells that expressed markers of NC-MSC lineage and pericytes and increased in frequency post-radiation, indicating that they may arise from different sub-populations. Lineage-tracing analysis using cell-type specific promoters also revealed that pericyte-like cells (DESMIN-mCherry) are distinct from EC-like cells (VE-CADHERIN-mCherry). In addition, sorted GEC and GPC fractions show key gene expression differences, with GPC expressing more mesenchymal gene signature in line with their mesenchymal origin, and GEC expressing more endothelial and angiogenic markers. Since radiation-induces Mesenchymal conversion of Proneural GSC, and our finding that Mesenchymal subtype of GBM exhibit greater propensity for pericyte transdifferentiation, it is possible that mesenchymal GSC acquire

a pericyte-like state by expressing markers such as DESMIN or αSMA, providing a rationale for their greater frequency in tumors compared to GEC.

Prior studies have indicated that glioma-derived endothelial cells, while relatively rare, can incorporate into the vasculature, although their role in carrying blood has not been proven (Ricci-Vitiani et al., 2010; Soda et al., 2011). Glioma-derived pericytes are more common and their functional roles in glioma progression have been more clearly defined (Cheng et al., 2013; Zhou et al., 2017). Our findings indicate that while radiation markedly enhances the frequency of GEC and GPC, these cells do not appear to incorporate into the vasculature to play an important role in carrying blood supply. Rather, our data suggest that these cells provide the remaining tumor cells with trophic support, allowing them to survive the severe stress of radiation. The concept of a “vascular niche” that provides trophic support is a common finding in stem cell biology. In the mammalian central nervous system, endothelial cells provide a niche that supports the survival and self-renewal capacity of neural stem cells (Shen et al., 2004). Studies in rodent models indicate that the vascular niche allows tumor cells to survive radiation-induced stress (Charles and Holland, 2010; Hambardzumyan and Bergers, 2015). Our results indicate that radiation may cause gliomas to, in fact, create their own supportive niche. The factor or factors elaborated by the radiation-induced GEC and GPC are yet to be elucidated, but will undoubtedly be the targets for potential therapeutic intervention.

Several independent studies have reported that GSC transdifferentiation into endothelial-like cells in tumors is mediated by factors such as HIF1A, NOTCH1, ETV2, WNT5A, TIE2 signaling, and pericyte-transdifferentiation of GSC via TGFβ signaling (Cheng et al., 2013; Deshors et al., 2019; Hu et al., 2016; Ricci-Vitiani et al., 2010; Soda et al., 2011; Wang et al., 2010; Zhao et al., 2018). Our transcriptomic analyses did not reveal significant enrichment of these factors in

either endothelial-like or pericyte-like clusters and tumor cells post-radiation suggesting that radiation-induced vascular transdifferentiation may occur via a different molecular mechanism.

Low- and high-dose radiation has been shown to alter histone gene expression and induce methylation changes in cell lines and in animal studies (Antwih et al., 2013; Jarah A. Meador et al., 2011). Because cell state transitions and phenotype switching requires alterations in the epigenome, we posited that epigenetic rewiring during DNA repair following radiation-induced damage may promote phenotype plasticity in glioma cells. Indeed, ATAC-sequencing results showed increased chromatin accessibility in vascular gene regions implying a role for epigenetic factors in driving this phenotype switch. Lysine acetylation of histones is an important post-translational modification that regulates chromatin accessibility (Görisch et al., 2005). Of all the histone acetyltransferase (HAT) genes, P300 was enriched in radiated tumor cells and transdifferentiated cells. Remarkably, blocking P300 HAT activity with C646, a selective small molecule inhibitor resulted in reduced vascular marker expression post-radiation. P300-deficient tumors showed reduced vascular transdifferentiation and tumor growth after radiation treatment, and improved animal survival. Collectively, our findings indicate that radiation reprograms glioma cells driving transdifferentiation to endothelial-like and pericyte-like cells, and targeting P300 with HAT inhibitors may be effective in preventing vascular transdifferentiation and tumor recurrence in GBM.

Experimental Procedures: See supplemental Information

Acknowledgements

The authors thank the UCLA pathology, flow cytometry, TCGB and UNGC sequencing cores for their technical assistance. S.M was funded by the Broad Stem cell postdoctoral fellowship, UCLA. H.K was funded by the Dr. Miriam and Sheldon G. Adelson Medical Research

Foundation, and the UCLA SPORE in Brain Cancer P50 CA211015-01A1. A.D was funded by R01HL149687.

Author contributions

S.M and H.K conceptualized, designed the experiments and wrote the manuscript. S.M, P.N, R.P, M.J, N.V, M.C, A.A, R.G, and Q.W conducted the experiments. R.K and Y.Q. performed the bioinformatics analysis. F.P, T.B, D.G, M.C, and P.L contributed resources and reagents. A.D, J.H, and S.G contributed valuable inputs in designing experiments and data analysis.

Declaration of Interests

The authors declare no competing interests

References:

Aldape, Kenneth, Kevin M. Brindle, Louis Chesler, Rajesh Chopra, Amar Gajjar, Mark R. Gilbert, Nicholas Gottardo, et al. 2019. “Challenges to Curing Primary Brain Tumours.” *Nature Reviews Clinical Oncology* 16 (8): 509–20.

Alexander, J.Jeffrey, Remedios Miguel, and Debra Graham. 1991. “Low Density Lipoprotein Uptake by an Endothelial-Smooth Muscle Cell Bilayer.” *Journal of Vascular Surgery* 13 (3): 444–51.

Antwih, Deborah A, Kristina M Gabbara, Wayne D Lancaster, Douglas M Ruden, and Steven P Zielske. 2013. “Radiation-Induced Epigenetic DNA Methylation Modification of Radiation-Response Pathways.” *Epigenetics* 8 (8): 839–48.

Armulik, Annika, Alexandra Abramsson, and Christer Betsholtz. 2005. “Endothelial/Pericyte Interactions.” *Circulation Research* 97 (6): 512–23.

Armulik, Annika, Guillem Genové, and Christer Betsholtz. 2011. “Pericytes: Developmental, Physiological, and Pathological Perspectives, Problems, and Promises.” *Developmental Cell* 21 (2): 193–215.

Auffinger, B, A L Tobias, Y Han, G Lee, D Guo, M Dey, M S Lesniak, and A U Ahmed. 2014. “Conversion of Differentiated Cancer Cells into Cancer Stem-like Cells in a Glioblastoma Model after Primary Chemotherapy.” *Cell Death & Differentiation* 21 (7): 1119–31.

Bannister, Andrew J, and Tony Kouzarides. 2011. “Regulation of Chromatin by Histone Modifications.” *Cell Research* 21 (3): 381–95.

Bhat, Kruttika, Mohammad Saki, Erina Vlashi, Fei Cheng, Sara Duhachek-Muggy, Claudia Alli, Garrett Yu, et al. 2020. “The Dopamine Receptor Antagonist Trifluoperazine Prevents Phenotype Conversion and Improves Survival in Mouse Models of Glioblastoma.” *Proceedings of the National Academy of Sciences* 117 (20): 11085.

Bhat, Krishna P.L., Veerakumar Balasubramaniyan, Brian Vaillant, Ravesanker Ezhilarasan, Karlijn Hummelink, Faith Hollingsworth, Khalida Wani, et al. 2013. “Mesenchymal Differentiation Mediated by NF-KB Promotes Radiation Resistance in Glioblastoma.” *Cancer Cell* 24 (3): 331–46.

Bowers, Erin M., Gai Yan, Chandrani Mukherjee, Andrew Orry, Ling Wang, Marc A. Holbert, Nicholas T. Crump, et al. 2010. “Virtual Ligand Screening of the P300/CBP Histone Acetyltransferase: Identification of a Selective Small Molecule Inhibitor.” *Chemistry & Biology* 17 (5): 471–82.

Brescia, Paola, Barbara Ortensi, Lorenzo Fornasari, Daniel Levi, Giovanni Broggi, and Giuliana Pelicci. 2013. “CD133 Is Essential for Glioblastoma Stem Cell Maintenance.” *STEM CELLS* 31 (5): 857–69.

Charles, N., Holland, E.C., 2010. The perivascular niche microenvironment in brain tumor progression. Cell Cycle 9, 3012–3021. https://doi.org/10.4161/cc.9.15.12710

Cheng, Lin, Zhi Huang, Wenchao Zhou, Qiulian Wu, Shannon Donnola, James K. Liu, Xiaoguang Fang, et al. 2013. “Glioblastoma Stem Cells Generate Vascular Pericytes to Support Vessel Function and Tumor Growth.” *Cell* 153 (1): 139–52.

Corces, M.R., Trevino, A.E., Hamilton, E.G., Greenside, P.G., Sinnott-Armstrong, N.A., Vesuna, S., Satpathy, A.T., Rubin, A.J., Montine, K.S., Wu, B., Kathiria, A., Cho, S.W., Mumbach, M.R., Carter, A.C., Kasowski, M., Orloff, L.A., Risca, V.I., Kundaje, A., Khavari, P.A., Montine, T.J., Greenleaf, W.J., Chang, H.Y., 2017. An improved ATAC-seq protocol reduces background and enables interrogation of frozen tissues. Nature Methods 14, 959–962. https://doi.org/10.1038/nmeth.4396

Dahan, P., J. Martinez Gala, C. Delmas, S. Monferran, L. Malric, D. Zentkowski, V. Lubrano, C. Toulas, E. Cohen-Jonathan Moyal, and A. Lemarie. 2014. “Ionizing Radiations Sustain Glioblastoma Cell Dedifferentiation to a Stem-like Phenotype through Survivin: Possible Involvement in Radioresistance.” *Cell Death & Disease* 5 (11): e1543–e1543.

De Pascalis, Ivana, Liliana Morgante, Simone Pacioni, Quintino Giorgio D’Alessandris, Stefano Giannetti, Maurizio Martini, Lucia Ricci-Vitiani, et al. 2018. “Endothelial Trans-Differentiation in Glioblastoma Recurring after Radiotherapy.” *Modern Pathology* 31 (9): 1361–66.

De Val, Sarah, and Brian L. Black. 2009. “Transcriptional Control of Endothelial Cell Development.” *Developmental Cell* 16 (2): 180–95.

DeCicco-Skinner, Katie L, Gervaise H Henry, Christophe Cataisson, Tracy Tabib, J Curtis Gwilliam, Nicholas J Watson, Erica M Bullwinkle, et al. 2014. “Endothelial Cell Tube Formation Assay for the in Vitro Study of Angiogenesis.” *Journal of Visualized Experiments : JoVE*, no. 91 (September): e51312–e51312.

Deshors, Pauline, Christine Toulas, Florent Arnauduc, Laure Malric, Aurore Siegfried, Yvan Nicaise, Anthony Lemarié, et al. 2019. “Ionizing Radiation Induces Endothelial

Transdifferentiation of Glioblastoma Stem-like Cells through the Tie2 Signaling Pathway." *Cell Death & Disease* 10 (11).

Francescone, Ralph A, 3rd, Michael Faibish, and Rong Shao. 2011. "A Matrigel-Based Tube Formation Assay to Assess the Vasculogenic Activity of Tumor Cells." *Journal of Visualized Experiments : JoVE*, no. 55 (September): 3040.

Görisch, Sabine M., Malte Wachsmuth, Katalin Fejes Tóth, Peter Lichter, and Karsten Rippe. 2005. "Histone Acetylation Increases Chromatin Accessibility." *Journal of Cell Science* 118 (24): 5825–34.

Hambardzumyan, D., Bergers, G., 2015. Glioblastoma: Defining Tumor Niches. Trends in cancer 1, 252–265. https://doi.org/10.1016/j.trecan.2015.10.009

Hingorani, M, W P Colley, S Dixit, and A M Beavis. 2012. "Hypofractionated Radiotherapy for Glioblastoma: Strategy for Poor-Risk Patients or Hope for the Future?" *The British Journal of Radiology* 85 (1017): e770–81.

Hu, Baoli, Qianghu Wang, Y. Alan Wang, Sujun Hua, Charles-Etienne Gabriel Sauvé, Derrick Ong, Zheng D. Lan, et al. 2016. "Epigenetic Activation of WNT5A Drives Glioblastoma Stem Cell Differentiation and Invasive Growth." *Cell* 167 (5): 1281-1295.e18.

Hu, Y., Smyth, G.K., 2009. ELDA: Extreme limiting dilution analysis for comparing depleted and enriched populations in stem cell and other assays. Journal of Immunological Methods 347, 70–78. https://doi.org/10.1016/j.jim.2009.06.008

Jarah A. Meador, Shanaz A. Ghandhi, and Sally A. Amundson. 2011. "P53-Independent Downregulation of Histone Gene Expression in Human Cell Lines by High- and Low-LET Radiation." *Radiation Research* 175 (6): 689–99.

Laks, D.R., Crisman, T.J., Shih, M.Y.S., Mottahedeh, J., Gao, F., Sperry, J., Garrett, M.C., Yong, W.H., Cloughesy, T.F., Liau, L.M., Lai, A., Coppola, G., Kornblum, H.I., 2016. Large-scale assessment of the gliomasphere model system. Neuro-Oncology 18, 1367–1378. https://doi.org/10.1093/neuonc/now045

Lathia, Justin D, Stephen C Mack, Erin E Mulkearns-Hubert, Claudia L L Valentim, and Jeremy N Rich. 2015. “Cancer Stem Cells in Glioblastoma,” *Genes & Dev*16: 1203-1217

Lau, Jasmine, Shirin Ilkhanizadeh, Susan Wang, Yekaterina A. Miroshnikova, Nicolas A. Salvatierra, Robyn A. Wong, Christin Schmidt, Valerie M. Weaver, William A. Weiss, and Anders I. Persson. 2015. “STAT3 Blockade Inhibits Radiation-Induced Malignant Progression in Glioma.” *Cancer Research* 75 (20): 4302–11.

Lee, Gina, Brenda Auffinger, Donna Guo, Tanwir Hasan, Marc Deheeger, Alex L. Tobias, Jeong Yeon Kim, et al. 2016. “Dedifferentiation of Glioma Cells to Glioma Stem-like Cells By Therapeutic Stress-Induced HIF Signaling in the Recurrent GBM Model.” *Molecular Cancer Therapeutics* 15 (12): 3064.

Minata, Mutsuko, Alessandra Audia, Junfeng Shi, Songjian Lu, Joshua Bernstock, Marat S. Pavlyukov, Arvid Das, et al. 2019. “Phenotypic Plasticity of Invasive Edge Glioma Stem-like Cells in Response to Ionizing Radiation.” *Cell Reports* 26 (7): 1893-1905.e7.

Ming-Tsang Chiao, Yi-Chin Yang, Wen-Yu Cheng, and Chiung-Chyi Shen and Jiunn-Liang Ko. 2011. “CD133+ Glioblastoma Stem-Like Cells Induce Vascular Mimicry in Vivo.” *Current Neurovascular Research* 8 (3): 210–19.

Neftel, Cyril, Julie Laffy, Mariella G. Filbin, Toshiro Hara, Marni E. Shore, Gilbert J. Rahme, Alyssa R. Richman, et al. 2019. “An Integrative Model of Cellular States, Plasticity, and Genetics for Glioblastoma.” *Cell* 178 (4): 835-849.e21.

Núñez, Felipe J., Flor M. Mendez, Padma Kadiyala, Mahmoud S. Alghamri, Masha G. Savelieff, Maria B. Garcia-Fabiani, Santiago Haase, et al. 2019. “IDH1-R132H Acts as a Tumor Suppressor in Glioma via Epigenetic up-Regulation of the DNA Damage Response.” *Science Translational Medicine* 11 (479): eaaq1427.

Osuka, Satoru, and Erwin G. Van Meir. 2017. “Overcoming Therapeutic Resistance in Glioblastoma: The Way Forward.” *The Journal of Clinical Investigation* 127 (2): 415–26.

Prager, Briana C., Shruti Bhargava, Vaidehi Mahadev, Christopher G. Hubert, and Jeremy N. Rich. 2020. “Glioblastoma Stem Cells: Driving Resilience through Chaos.” *Trends in Cancer* 6 (3): 223–35.

Reik, Wolf, Wendy Dean, and Jörn Walter. 2001. “Epigenetic Reprogramming in Mammalian Development.” *Science* 293 (5532): 1089.

Ricci-Vitiani, Lucia, Roberto Pallini, Mauro Biffoni, Matilde Todaro, Gloria Invernici, Tonia Cenci, Giulio Maira, et al. 2010. “Tumour Vascularization via Endothelial Differentiation of Glioblastoma Stem-like Cells.” *Nature* 468 (7325): 824–28.

Shen, Q., Goderie, S.K., Jin, L., Karanth, N., Sun, Y., Abramova, N., Vincent, P., Pumiglia, K., Temple, S., 2004. Endothelial Cells Stimulate Self-Renewal and Expand Neurogenesis of Neural Stem Cells. Science 304, 1338. https://doi.org/10.1126/science.1095505

Soda, Yasushi, Tomotoshi Marumoto, Dinorah Friedmann-Morvinski, Mie Soda, Fei Liu, Hiroyuki Michiue, Sandra Pastorino, et al. 2011. “Transdifferentiation of Glioblastoma Cells into Vascular Endothelial Cells.” *Proceedings of the National Academy of Sciences* 108 (11): 4274.

Suvà, Mario L., Nicolo Riggi, and Bradley E. Bernstein. 2013. “Epigenetic Reprogramming in Cancer.” *Science* 339 (6127): 1567.

Wang, Rong, Kalyani Chadalavada, Jennifer Wilshire, Urszula Kowalik, Koos E. Hovinga, Adam Geber, Boris Fligelman, Margaret Leversha, Cameron Brennan, and Viviane Tabar. 2010. “Glioblastoma Stem-like Cells Give Rise to Tumour Endothelium.” *Nature* 468 (7325): 829–33.

Yuan, Salina, Robert J. Norgard, and Ben Z. Stanger. 2019. “Cellular Plasticity in Cancer.” *Cancer Discovery* 9 (7): 837–51.

Zhao, Chengjian, Gustavo A Gomez, Yuwei Zhao, Yu Yang, Dan Cao, Jing Lu, Hanshuo Yang, and Shuo Lin. 2018. “ETV2 Mediates Endothelial Transdifferentiation of Glioblastoma.” *Signal Transduction and Targeted Therapy* 3:4

Zhou, Wenchao, Cong Chen, Yu Shi, Qiulian Wu, Ryan C. Gimple, Xiaoguang Fang, Zhi Huang, et al. 2017. “Targeting Glioma Stem Cell-Derived Pericytes Disrupts the Blood-Tumor Barrier and Improves Chemotherapeutic Efficacy.” *Cell Stem Cell* 21 (5): 591-603.e4.

Figure Legends

Figure 1: Single-cell sequencing reveals diverse functional states of radiated glioma cells

(A) UMAP plots show clustering of glioma cells from control (0 Gy) and 2-days and 7-days radiated (8 Gy) fractions.

(B) Histogram shows the number of cells per cluster in each group.

(C) Heatmap shows Louvain clustering and EnrichR gene modules in each cluster. Clusters 0 and 4 are highlighted in red, along with their enriched modules.

(D) UMAP plot of pseudotime trajectory analysis. Clusters 0 and 4 are highlighted in red.

(E) Heatmap shows normalized enrichment score (NES) of gene sets in glioma cells 2- and 7-days post-radiation.

(F) Graph shows LogFc expression of genes in the GO: Angiogenesis category in radiated vs control glioma cells.

(G) Heatmap shows relative expression of endothelial, pericyte and stemness genes in control and radiated glioma cells. N=3, *, ** indicates $p<0.05$, and $p<0.005$, two-tailed t-test. See also Figure S1.

Figure 2: Radiation promotes endothelial and pericyte marker expression in glioma cells

(A) Heatmap shows relative expression of endothelial, pericyte, stemness and EMT genes in control (0 Gy), fractionated (2 Gy X4) and single dose (8 Gy) radiated glioma cells.

(B) Heatmap shows relative expression of endothelial, pericyte and stemness markers in control and radiated glioma cells from multiple patient-derived gliomasphere lines.

(C, D) Representative images of mCherry expression in control and radiated cells. Graph shows flow-cytometric quantitation of percentage of mCherry+ cells in each condition.

(E) Heatmap shows relative expression of endothelial, pericyte and stemness genes in CD133+ (GSC) and CD133- (non-GSC) fractions 3- and 7-days post-radiation.

(F) Immunostaining images of endothelial (CD31, CD144/VE-CADHERIN) and pericyte (DES, aSMA) markers in control and radiated CD133+ (and CD133- fractions of glioma cells. Scale bars, 50μm.

(G) Flow cytometric quantitation of percentage of mCherry+ cells in control and radiated CD133+ and CD133- fractions.

(H) Immunostaining images of VE-CADHERIN and DESMIN markers in GFP+ tumor cells in control and radiated tumor xenografts. Scale bars, 50μm. White arrows point to GFP+ marker+ cells in each image.

(I,J) Immunostaining images of mCherry and GFP in control and radiated tumor xenografts. Graph shows flow-cytometric quantitation of percentage of mCherry+ cells normalized to total number of GFP+ tumor cells in each group. N=2, and ** indicates $p<0.005$ derived from Welchs t-test. Scale bars, 100μm

(K, L) Immunostaining images of VE-CADHERIN and DESMIN in GFP+ tumor cells in mouse GBM model. Arrows point to marker+ GFP+ cells in each group. Scale bars, 50μm. Graphs show quantitation of number of GFP+ marker+ cells in blood vessel (BV) and tumor mass.N=3, * and *** indicates $p<0.05$ and $p<0.0005$ derived from Welchs t-test.

Error bars represent s.d. of the mean in (D, G), N=3, * and ** indicates $p<0.05$ and $p<0.005$, two-tailed t-test. See also Figure S2.

Figure 3: iGEC display typical characteristics of normal vascular endothelial cells

(A-D) Tubular network formation on matrigel and immunostaining of VE-CADHERIN and Di-AcLDL in control and radiated glioma cells. Scale bars, 100μm. Graphs show quantitation of

branch points and number of Di-Ac-LDL+ cells per field in each group. Error bars represent mean±SD, and * and ** indicates p<0.05 and p<0.005, Welchs t-test.

(E) Schematic outlines the matrigel plug in vivo angiogenesis assay.

(F) Images show H&E and Masson's trichrome staining. Scale bars, 500μm. Representative images of immunostaining of mCherry (GEC, red), GFP (tumor cells, green) and Tomato Lectin (vessels, grey). Scale bars, 20μm.

(G) Graph shows quantitation of vessel density in each group. Error bars represent mean ± SD and *, ** indicates p<0.05 and p<0.005, two-tailed Students t-test.

(H) MDS plot shows clustering of tumor and transdifferentiated cells.

(I) Heatmap shows NES of gene sets in each group. See also Figure S3.

Figure 4: iGEC and iGPC promote tumor growth post-treatment

(A) Schematic outlines the conditioned media (CM) and co-transplantation tumor growth experiments.

(B) Graph shows quantitation of proliferation of control and radiated tumor cells in GEC and GPC conditioned media (CM). Error bars represent mean±SD, N=3, and *, ** indicates p<0.05 and p<0.005, two-tailed t-test.

(C,D) Images of mice showing tumor growth at 2 and 4 weeks. Box plots show quantitation of tumor growth by luminescence in each group. N=5 mice per group and * indicates p<0.05, one-way ANOVA and post-hoc t-test.

(E) Kaplan-meier survival curve of mice transplanted with tumor cells and GEC/GPC. * and ** indicates p<0.05 and p<0.005, Log-rank test.

(F) Schematic outlines the depletion of GEC/GPC using HSV-TK method in tumor xenografts

(G,H) Images of mice showing tumor growth at 2 and 4 weeks. Box plots show the quantitation of tumor growth by luminescence. * indicates p-value <0.05 and n.s. not significant, one-way ANOVA and post-hoc t-test. See also Figure S4.

Figure 5: Radiation alters chromatin accessibility in vascular gene regions

(A) Total peak count of control and radiated gliomaspheres. ***** indicates $p<0.05$, two-tailed t-test.

(B) Pie chart shows the number of peaks shared and unique to control and radiated cells.

(C) Graph shows peak distribution in various genomic regions in control and radiated cells.

(D) Peak size differences in promoter and intergenic regions in endothelial (CDH5, PECAM1) and pericyte (MCAM, ANGPT1) genes

(E) Table shows motifs of vascular specification transcription factors enriched in radiated gliomaspheres.

(F) Graph shows percentage of sequences containing the motifs significantly enriched in radiated gliomaspheres.

(G) Gene ontology analysis shows enrichment of vascular and blood vessel development related gene terms in radiated gliomaspheres. See also Figure S5.

Figure 6: Radiation increases histone acetylation and blocking P300 HAT activity inhibits vascular transdifferentiation

(A, B) Immunoblot images of total and Ac-histone 3 (AcH3, Lysine K27) in control and radiated cells. Quantitation of protein levels normalized to Actin is shown in the graph, N=2 and * indicates $p<0.05$, two-tailed t-test.

(C, D) Immunostaining images of Total H3 (red), AcH3 (red) and GFP (green) in control and radiated tumor xenografts. Quantitation of percentage of positive cells is shown in the graph, N=3 and * indicates $p<0.05$, two-tailed t-test.

(E) Heatmap shows LogFc expression of HAT transcripts in cultured control and radiated gliomaspheres. EP300 is highlighted in red.

(F) Immunoblot images of Total and AcH3 in DMSO and C646 treated gliomaspheres. Quantitation of protein level is shown in the graph. N=2, and * indicates $p<0.05$, two-tailed t-test.

(G) Quantitative RT-PCR analysis of endothelial, pericyte and stem genes in control and radiated gliomaspheres treated with C646 and DMSO. Error bars represent mean±SD, N=3, and * indicates $p<0.05$, two-tailed t-test.

(H, I) Images of mCherry expression in control and radiated cells treated with C646. Flow-cytometric quantitation of percentage of mCherry+ cells in each group is shown in the graph. * indicates $p<0.05$, N=3, two-tailed t-test.

(J) Heatmap of LogFC expression of endothelial, pericyte and stemness genes in control and radiated gliomaspheres treated with and without C646.

(K, M) Heatmap of NES of gene sets in control and radiated glioma cells treated with and without C646. See also Figure S6.

Figure 7: EP300-deficient glioma cells show reduced vascular transdifferentiation and tumor growth post-treatment

(A, B) Immunoblot images of total and AcH3 in EP300-deficient (siEP300) and control (siCTL) cells. Quantitation of protein levels is shown in the graph. N=2, and * indicates $p<0.05$, two-tailed t-test.

(C) Quantitative RT-PCR analysis of endothelial, pericyte and stem genes in EP300 deficient and control cells post- radiation. N=3, and * indicates $p<0.05$, two-tailed t-test.

(D, E) Images show mCherry expression in EP300-deficient and control cells post-radiation. Flow-cytometric quantitation of percentage of mCherry+ cells in each group is shown in the graph. N=3, * indicates $p<0.05$, two-tailed t-test.

(F) Graph shows quantiation of tumor growth pre- (Pre-Tx) and post-radiation (Post-Tx) treatment. N=5 mice per group, and ** indicates $p<0.005$, one-way ANOVA, post-hoc t-test.

(G) Kaplan-meier survival curve of mice pre- (Pre-Tx) and post-radiation treatment (Post-Tx). * and *** indicates $p<0.05$, and $p<0.0005$, Log-rank t-test.

(H) Immunostaining images VE-CADHERINDESMIN in GFP+ tumor cells. Arrows point to marker+ GFP+ cells in each group. Scale bars, 50μm. Quantitation of GFP+marker+ cells in tumor mass is shown in the graph. N=5 mice per group. Error bars represent mean ± sd, and * indicates $p < 0.05$, two-tailed t-test. See also Figure S7.

Figure 1:

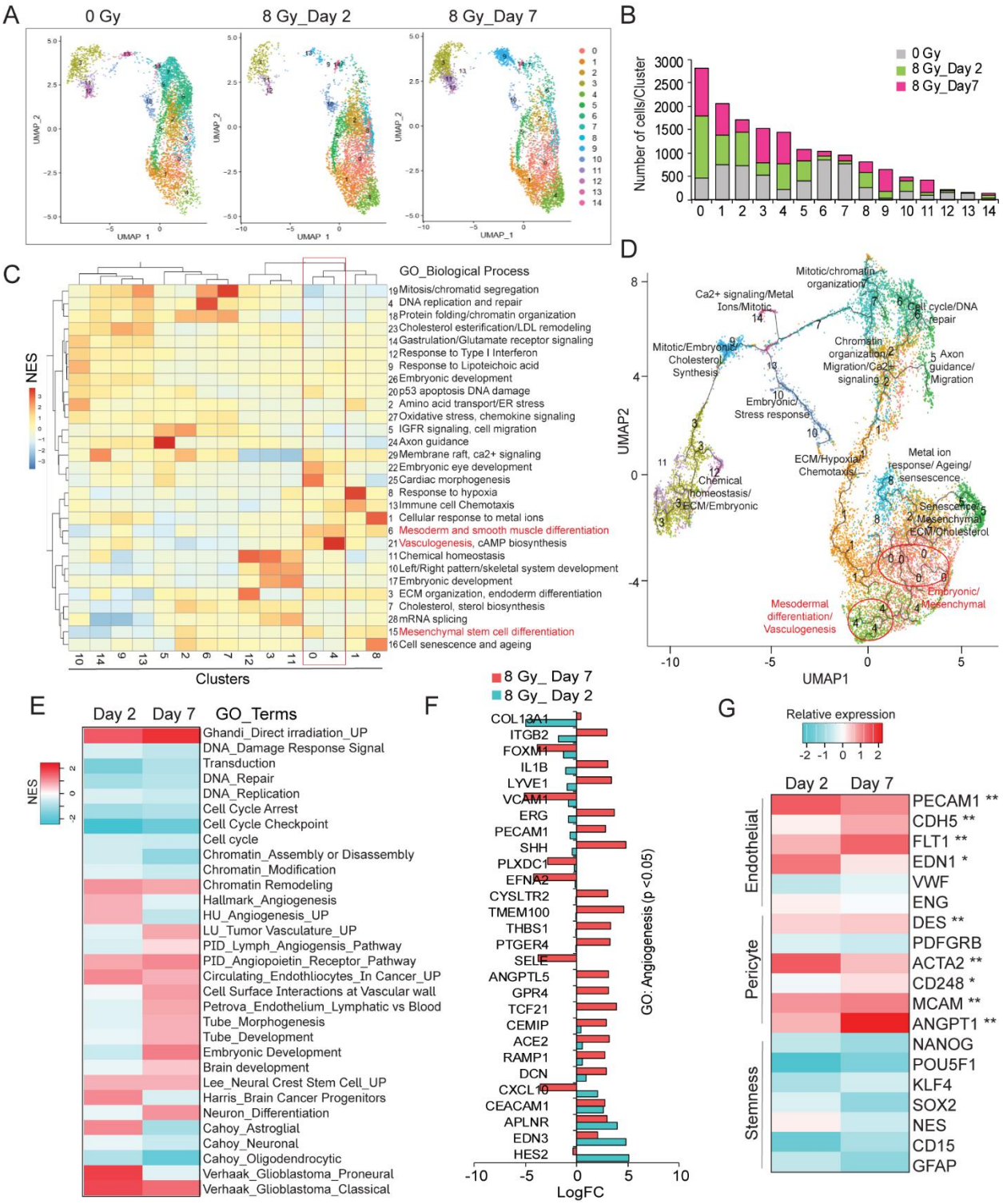

Figure 2:

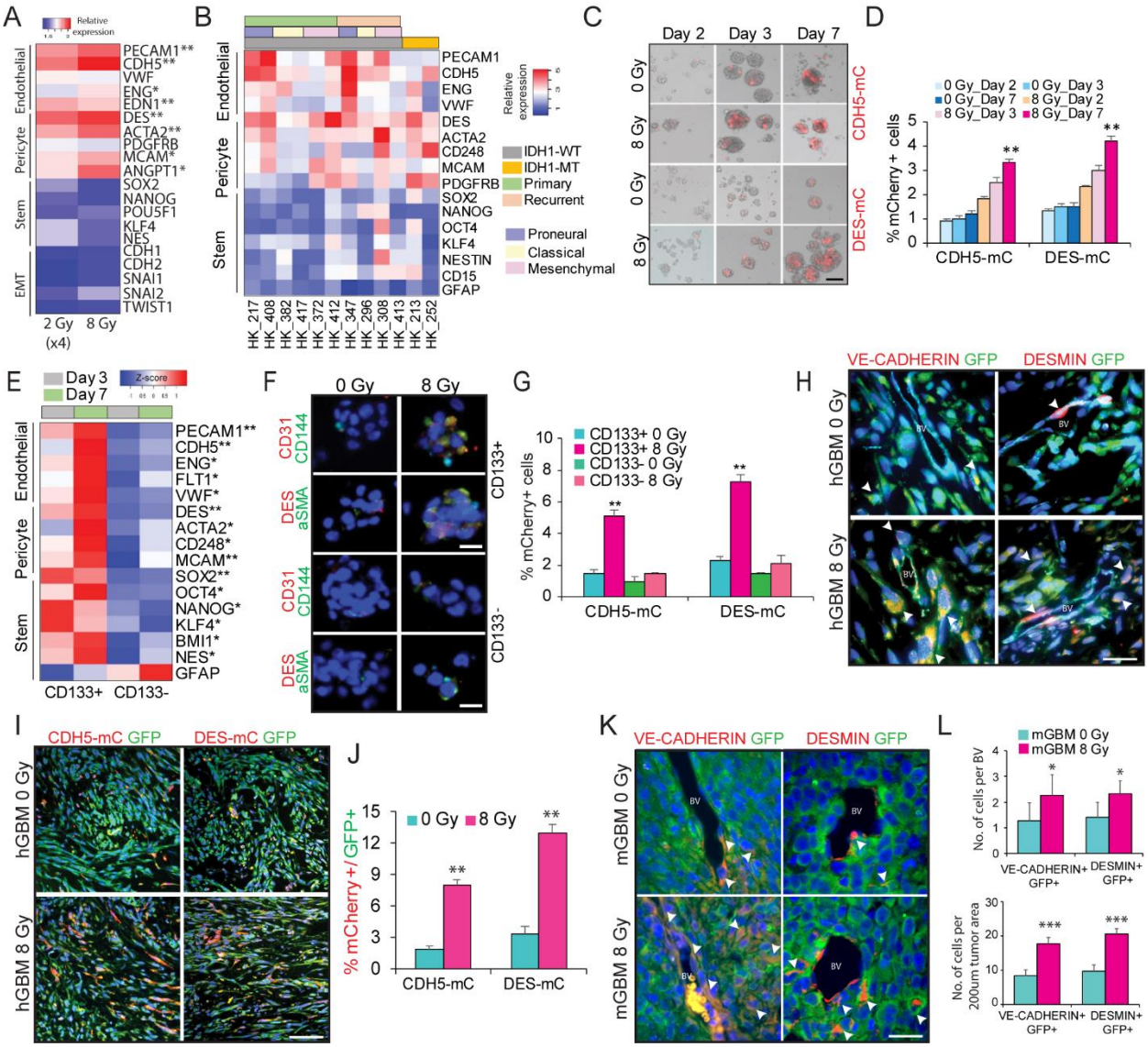

Figure 3:

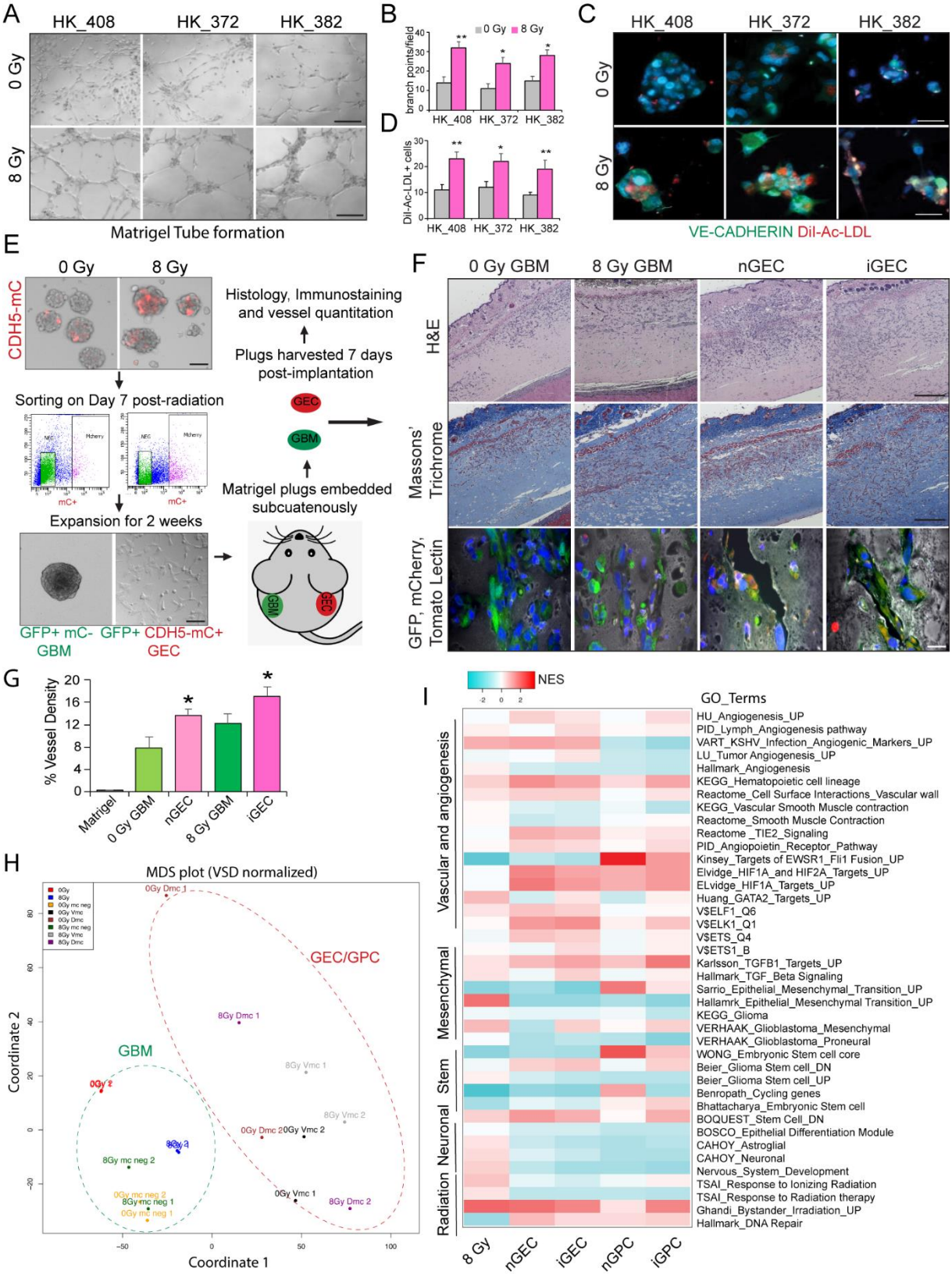

Figure 4:

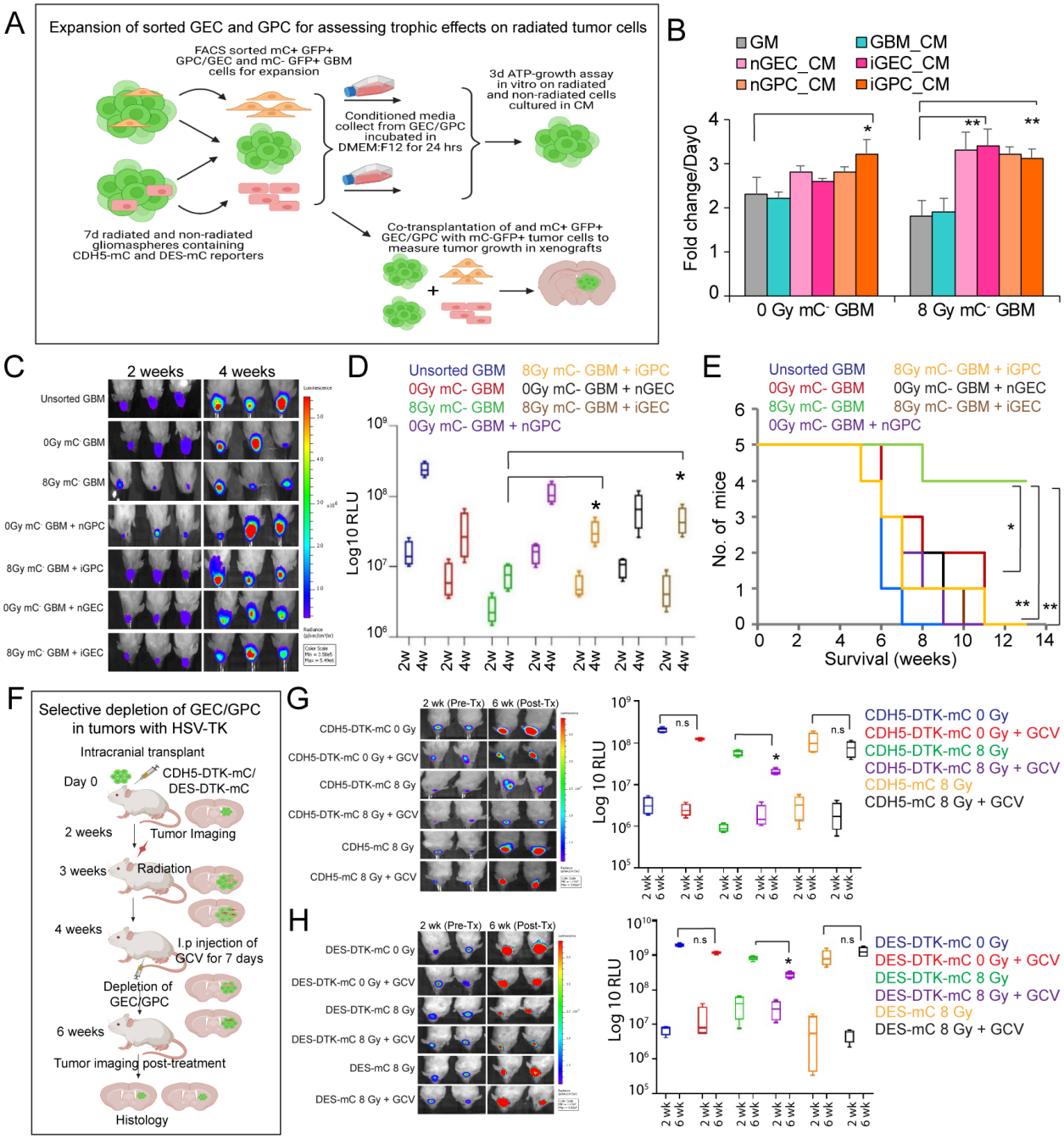

Figure 5:

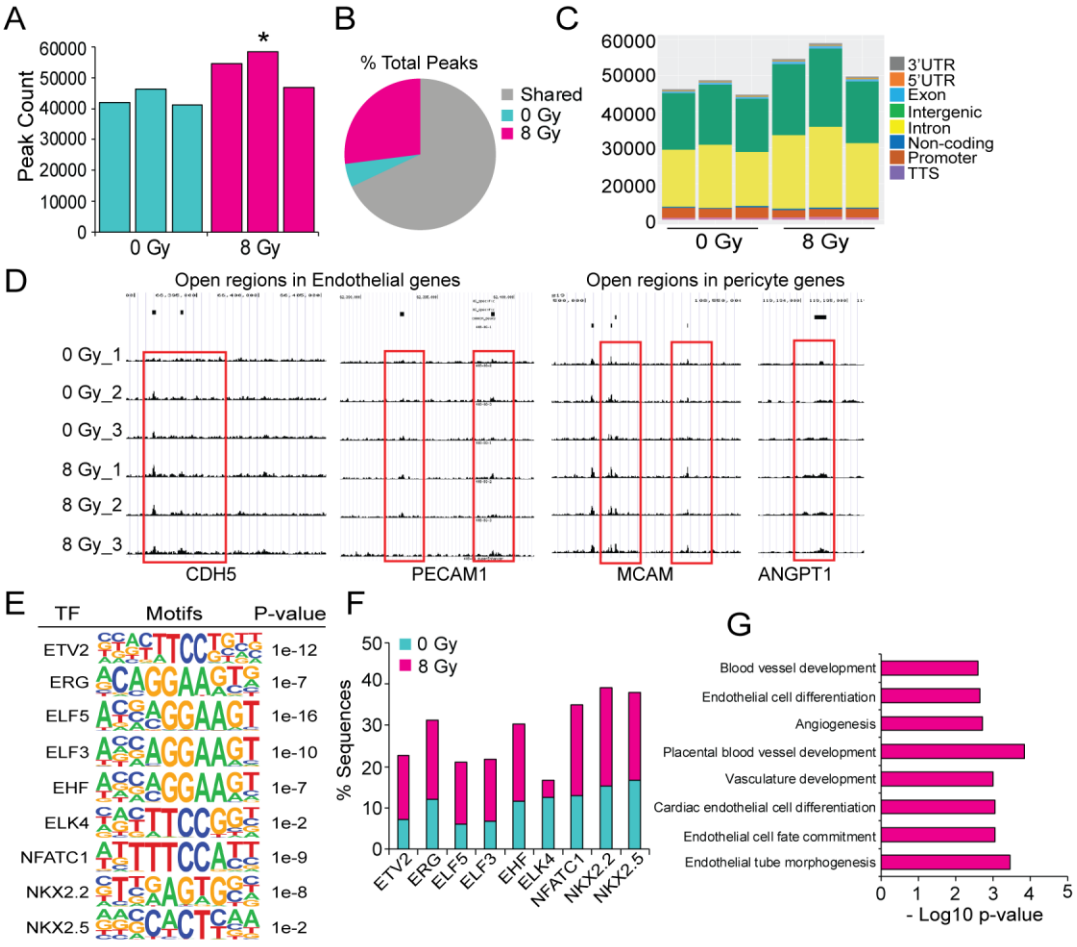

Figure 6:

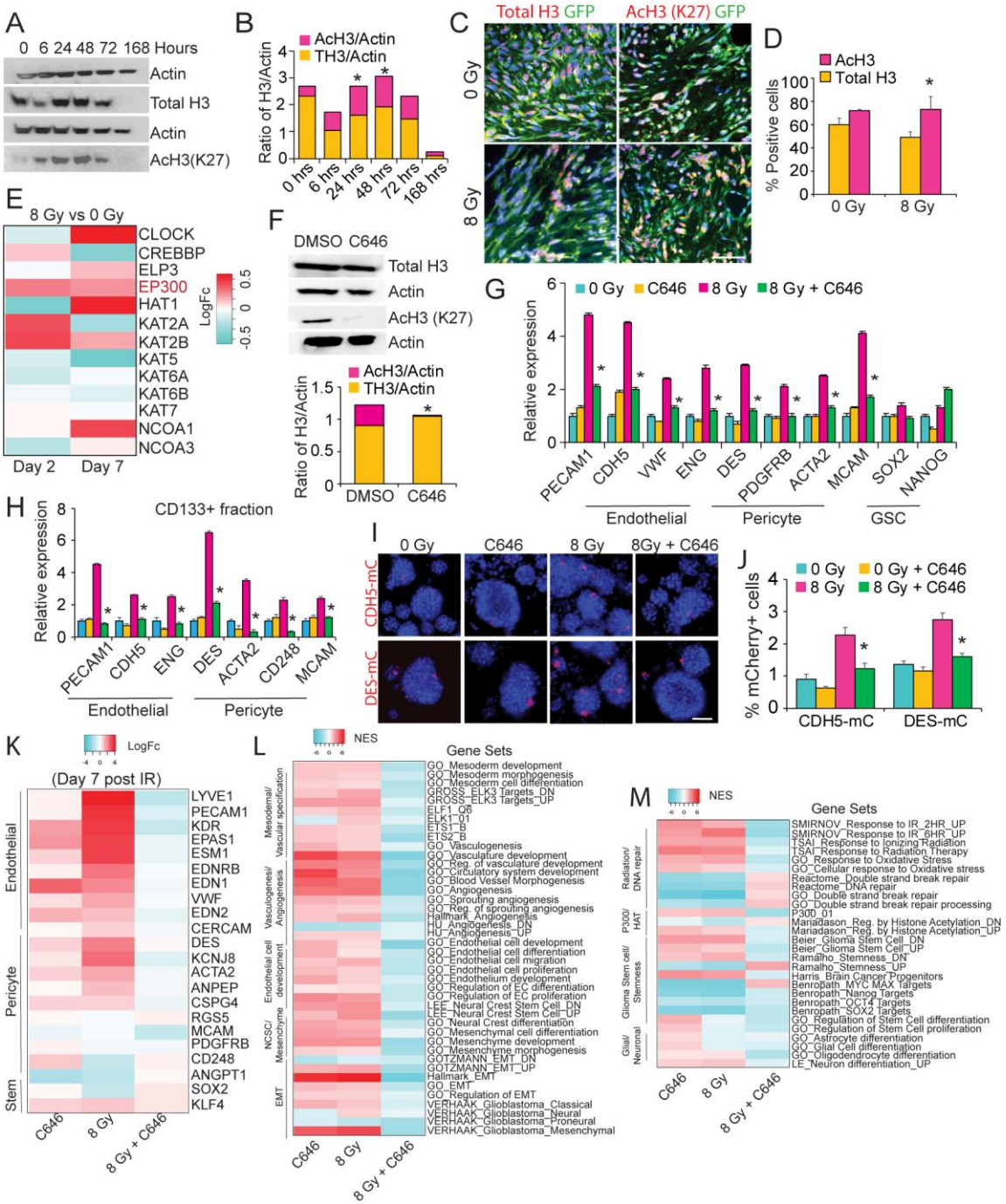

Figure 7: